In vitro model that approximates retinal damage threshold trends

Michael L. Denton
Michael S. Foltz
Kurt J. Schuster
Gary D. Noojin
Northrop Grumman
Warfighter Concepts and Applications Department
San Antonio, Texas

Larry E. Estlack
Conceptual MindWorks, Inc.
San Antonio, Texas

Robert J. Thomas
Air Force Research Laboratory
711 HPW/RHDO
Brooks City-Base, Texas

Abstract. Without effective *in vitro* damage models, advances in our understanding of the physics and biology of laser-tissue interaction would be hampered due to cost and ethical limitations placed on the use of nonhuman primates. We extend our characterization of laser-induced cell death in an existing *in vitro* retinal model to include damage thresholds at 514 and 413 nm. The new data, when combined with data previously reported for 532 and 458 nm exposures, provide a sufficiently broad range of wavelengths and exposure durations (0.1 to 100 s) to make comparisons with minimum visible lesion (*in vivo*) data in the literature. Based on similarities between *in vivo* and *in vitro* action spectra and temporal action profiles, the cell culture model is found to respond to laser irradiation in a fundamentally similar fashion as the retina of the rhesus animal model. We further show that this response depends on the amount of intracellular melanin pigmentation.
[DOI: 10.1117/1.2981831]

Keywords: retinal pigment epithelia; damage threshold; action spectra; temporal action profile; *in vitro* model; Probit.

Paper 07372RR received Sep. 11, 2007; revised manuscript received Mar. 21, 2008; accepted for publication Apr. 28, 2008; published online Sep. 22, 2008. This paper is a revision of a paper presented at the SPIE Conference on Optical Interactions with Tissue and Cells XVIII, January 2007, San Jose, California. The paper presented there appears (unrefereed) in SPIE Proceedings Vol. 6435.

1 Introduction

There is an increasing demand for alternative models of analysis for laser bioeffects. Although assessment of ocular damage in nonhuman primate (NHP) models (*in vivo*) remains critical for providing guidelines for eye-safe exposures in humans, cost, availability, and ethical constraints on their use have hampered advances in the field of laser-tissue interaction. *In vitro* models must be validated by showing that they follow or predict the same basic trends between dosimetry and cell damage described in the NHP model. Computer simulation programs and cell culture systems (*in vitro*) are models that can provide important information about laser bioeffects. The simple and flexible nature of cell culture systems is ideal for providing rapid feedback to the modeling community regarding basic cellular response to lasers. In this unified experimental and mathematical model scenario, testing of novel lasers and discovery of new concepts (physics and biology) could initially be performed using an iterative approach between cell exposures and simulations before final validation in the NHP model, thus minimizing the use of animals.

Data from *in vivo* studies have shown that laser damage in the retina depends on wavelength, power density, and duration of the exposure.[1] Damage has been defined as the minimum irradiance leading to a visible lesion,[1,2] or by the statistical method of Probit,[3,4] which correlates laser dose and the probability of achieving a damaging event. The Probit estimated dose for 50% lethality (ED_{50}) is often defined as the damage threshold, which can be compared over a range of wavelengths (action spectrum) or exposure durations (temporal action profile) to identify trends in damage efficacy. We have previously described and reported ED_{50} damage thresholds in a human retinal pigment epithelial (RPE) cell model in which the sensitivity of the cells depends on the number of intracellular melanosome particles (MPs).[5–7] Here, we provide additional *in vitro* ED_{50} data that, when combined with our previous work, are presented as action spectra and temporal action profiles over four wavelengths and four exposure durations. Further, we compare our *in vitro* threshold data to those reported in the literature for minimum visible lesions in the NHP model.

2 Experimental

The materials and methods used to generate ED_{50} values in this report (514 and 413 nm), including the use of the same batch of isolated melanosomes, were identical to those used previously,[6] and thus, all data described here are comparable. Artificial pigmentation of hTERT-RPE1 cells (in 96-well microtiter plates) was carried out using volumes of stock MPs corresponding to equivalents of either 160 or 1600 particles per cell. Laser delivery to the RPE cells is shown in Fig. 1. For our experiments, the Millennia Pro (Spectra Physics, Irv-

Address all correspondence to Dr. Robert J. Thomas, 2650 Louis Bauer Drive, Brooks City-Base, Texas 78235. Tel: 210-536-6558; Fax: 210-536-3903; E-mail: robert.thomas@brooks.af.mil.

1083-3668/2008/13(5)/054014/6/$25.00 © 2008 SPIE

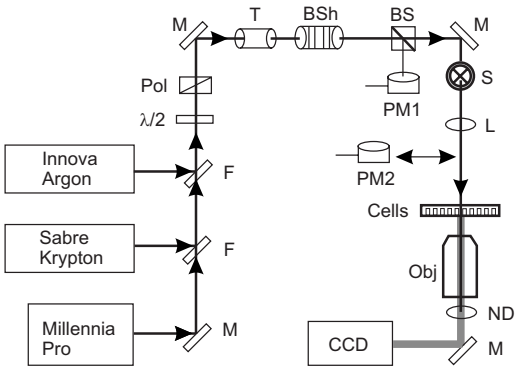

Fig. 1 Laser delivery for *in vitro* damage threshold experiments. M, mirror; F, flip-up mirror; Pol, polarizing cube; T, optical telescope; BSh, beam shaper; S, mechanical shutter; L, lens; PM, power meter; ND, neutral density filter; CCD, charge-coupled device camera; Obj, microscope objective. Details are found in Ref. 6.

ine, California) supplied the 532-nm light, and the Innova large-frame argon (Coherent Inc., Santa Clara, California) laser provided light of 514 and 458 nm. For exposures at 413 nm, the Sabre large-frame krypton laser (Coherent) was used. All beams were co-aligned to a common optical path using apertures and a flip-up mirror (F). Attenuation of laser power was achieved by the combination of a half-wave plate ($\lambda/2$) and polarizing beamsplitter (Pol). The optical path included a telescope (T), a beam shaper (BSh, model GBS-AR14, Newport Corp., Irvine, California), a computer-controlled shutter (S), and a single lens (L) imaging system (88-mm focal length) generating a beam diameter of about 250 μm at the cells. The telescope allowed for collimated beam expansion to 4.7 mm prior to entry into the beam shaper, which converted the beam to a flat-top profile. The imaging system was designed to image the beam at the near-field output of the beam shaper (8 mm diameter) via 0.05× magnification. The effect of the column of Hank's balanced salt solution above the cells during exposure was taken into account when identifying the laser beam diameter (knife-edge method).

Uncertainty in our irradiance values was determined from calculated combined standard uncertainties (types A and B) for measuring both laser power and diameter at the sample.[6] Damage threshold irradiance values (ED_{50}) were determined using the Probit[4] method. The Probit output includes additional uncertainty intervals (fiducial limits) related to the ED_{50} value, for which 95% confidence levels were used.

3 Results and Discussion

In vitro damage threshold values for all four wavelengths are summarized in Tables 1 and 2. Although experimental uncertainty in irradiance varied depending upon the power detector used, the maximum extended uncertainty of our ED_{50} values was 20% with an overall average of 14%. The Probit slope reported is the first derivative of the Probit curve at the ED_{50} value.

Trends in the ED_{50} data found in Tables 1 and 2 are summarized as action spectra (Fig. 2) and temporal action profiles (Fig. 3). It is apparent from both types of analyses that there was a pigment-dependent effect on the trends for the data. The

Table 1 Threshold ED_{50} values for laser exposures to the *in vitro* retinal model using 160 MPs/cell.

	0.1-s Exposures					1.0-s Exposures					10-s Exposures					100-s Exposures				
			Radiant Exposure ED_{50} (J/cm^2)					Radiant Exposure ED_{50} (J/cm^2)					Radiant Exposure ED_{50} (J/cm^2)					Radiant Exposure ED_{50} (J/cm^2)		
λ (nm)	n	Irrad. ED_{50} (W/cm^2)	ED_{50}	LFL–UFL	Slope	n	Irrad. ED_{50} (W/cm^2)	ED_{50}	LFL–UFL	Slope	n	Irrad. ED_{50} (W/cm^2)	ED_{50}	LFL–UFL	Slope	n	Irrad. ED_{50} (W/cm^2)	ED_{50}	LFL–UFL	Slope
532	19	664	66	50–74	31.0	23	508	508	403–622	12.3	25	347	3472	2608–4611	11.9	58	194	19417	16667–22278	7.8
514	71	463	46	43–50	16.7	60	292	292	283–311	44.2	48	215	2150	1890–2477	24.0	72	124	12363	10675–13569	8.8
458	58	479	48	42–55	11.6	44	305	305	264–391	6.2	46	250	2502	2245–2973	13.0	63	53	5266	3905–6122	8.8
413	48	404	40	34–46	14.2	48	320	320	286–352	13.4	48	192	1924	1156–2324	7.0	57	20	2040	1416–2637	4.2

Lower and upper fiducial limits (LFL and UFL) correspond to 95% confidence intervals. Probit slope represents the first derivative of the probit curve at the ED_{50} value. The total number of exposures (n) for each data set is provided.

Table 2 Threshold ED_{50} values for laser exposures to the *in vitro* retinal model using 1600 MPs/cell.

	1.0-s Exposures					10-s Exposures					100-s Exposures				
			Radiant Exposure ED_{50} (J/cm^2)					Radiant Exposure ED_{50} (J/cm^2)					Radiant Exposure ED_{50} (J/cm^2)		
λ (nm)	*n*	Irrad. ED_{50} (W/cm^2)	ED_{50}	LFL–UFL	Slope	*n*	Irrad. ED_{50} (W/cm^2)	ED_{50}	LFL–UFL	Slope	*n*	Irrad. ED_{50} (W/cm^2)	ED_{50}	LFL–UFL	Slope
532	58	59	59	51–69	14.1	100	50	503	422–572	24.4	48	33	3333	2806–4028	17.3
514	48	59	59	55–74	8.9	48	37	370	303–432	9.3	47	32	3178	2543–3683	11.5
458	39	73	73	61–84	12.2	41	53	526	446–605	33.5	48	43	4264	3736–4760	11.5

Lower and upper fiducial limits (LFL and UFL) correspond to 95% confidence intervals. Probit slope represents the first derivative of the probit curve at the ED_{50} value. The total number of exposures (*n*) for each data set is provided.

consequence of having approximately 10 times the number of melanosomes within each cell was an enhanced sensitivity to laser exposure. The effect, reported as fold reduction in ED_{50} (Table 3 of Ref. 6), was most pronounced for exposures presumed to produce damage by photothermal mechanisms, namely 0.1-s exposure at 532 nm. The ED_{50} values for 514 nm (new data) follow the same pigment-dependent trend as 532 and 458 nm, falling between the 532 and 458-nm ratios.

The irradiance action spectra for the 160-MPs/cell thresholds [Fig. 2(a)] show a substantial increase in cellular sensitivity (larger inverse irradiance) for cells exposed for 100 s at 413 nm, relative to the other wavelengths and exposure durations. Each of the lines generated from the 0.1-to 10-s data had a negative slope, indicating increased damage sensitivity at the shorter wavelengths. Additionally, for each of the wavelengths tested, there was increased damage sensitivity as exposure duration was increased. Both of these trends were also apparent in the *in vivo* data from Ham et al.,[2] which have been summarized in Fig. 2(c). Notice the increasing sensitivity of the rhesus retina at the shorter wavelengths and the longer exposure durations within a given wavelength.

The threshold data for cells with the higher pigmentation [Fig. 2(b)] also showed increased damage sensitivity as exposure duration was lengthened for each wavelength, but the magnitude of this effect was very minimal for the 100-s data [compare in Figs. 2(a) and 2(b) the 10-s and 100-s thresholds at 458 nm]. The slopes of the lines generated in the action spectra in Fig. 2(b) were positive, indicating a different trend relative to the *in vivo* data. Thus, even though the ED_{50} irradiance values for cells with the higher pigmentation were closer to the absolute values of the thresholds from Ham et al.,[2] the wavelength dependent trend in thresholds was lost.

Figure 3(a) relates our *in vitro* damage thresholds (radiant exposure) to exposure duration for each of the wavelengths using temporal action profiles. Although it was apparent that cells with greater pigmentation were more sensitive to the laser exposure, there was little distinction between the trend lines within each pigmentation data set when plotted on log-log axes. The *in vitro* ED_{50} trends at 514 and 413 nm followed the trends previously shown for 532 and 458 nm,[6] respectively. The trend for both 532 and 514 nm continued beyond 10-s exposure duration as a power function (Table 3). The ED_{50} values for exposure of cells containing 160 MPs at 458 and 413 nm trended together with the 532 and 514-nm data between 0.1 and 10 s (Table 3) but then deviated to a trend that was more horizontal. This transition appears to approximate the transitions seen in Fig. 3(b), where there was nearly constant threshold radiant exposure over time (irradiance reciprocity). Due to both a shift downward in thresholds relative to the longer wavelengths and a different break-off

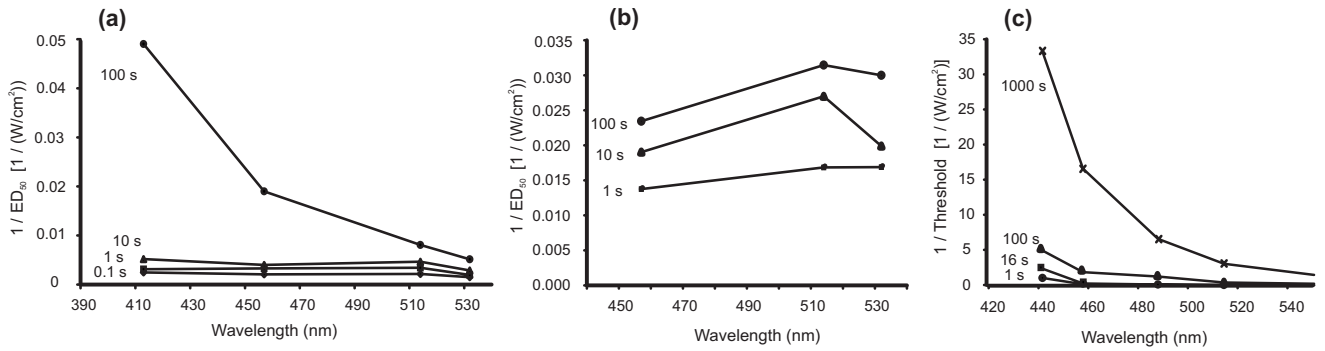

Fig. 2 Action spectra (inverse irradiance thresholds) for laser damage in the *in vitro* retinal model using (a) 160 MPs/cell or (b) 1600 MPs/cell, and in (c) the rhesus animal model (data taken from Ref. 2).

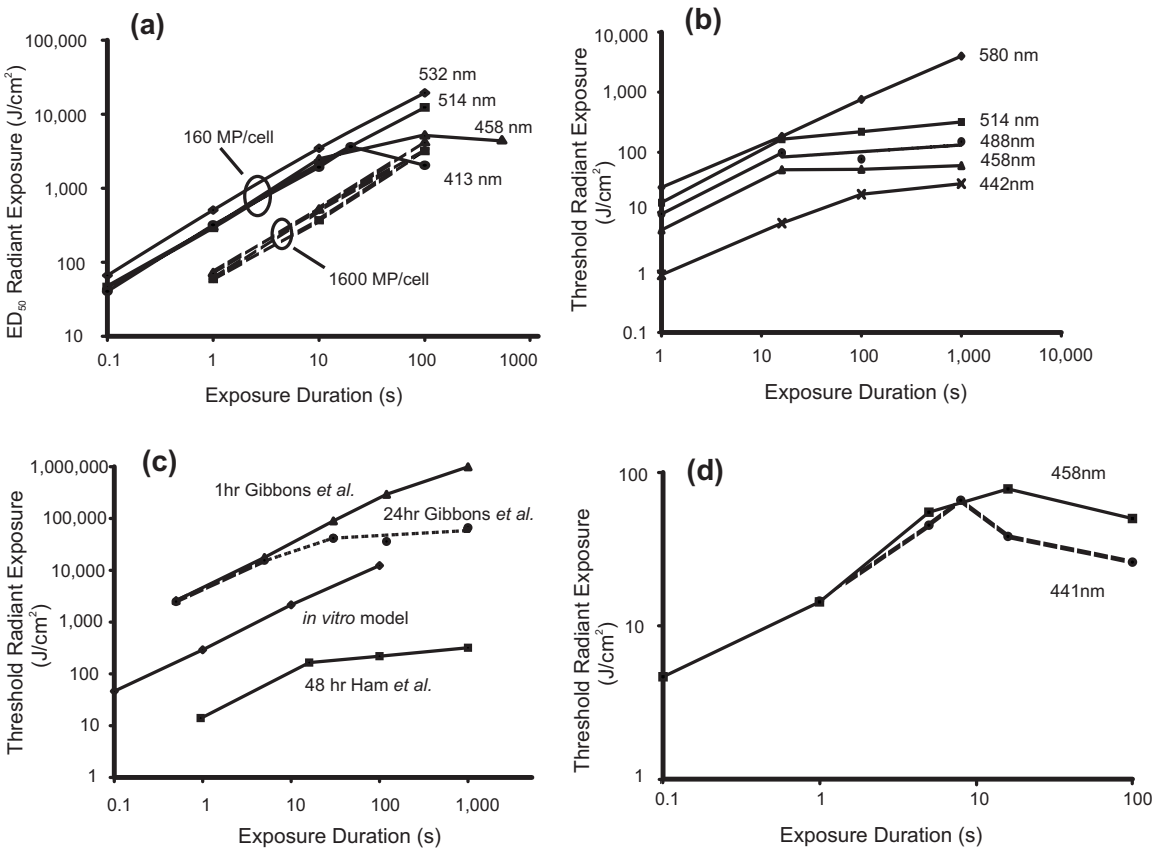

Fig. 3 Temporal action profiles for laser damage in (a) the *in vitro* retinal model, (b) the rhesus model (data taken from Ref. 2). (c) Comparison of *in vitro* and *in vivo* temporal action profiles for laser damage at 514 nm. Rhesus data taken from Ref. 2 (0.5-mm beam diameter and 48-h post-exposure damage assessment) and Ref. 8 (0.05-mm retinal beam diameter and either 1-h or 24-h post-exposure damage assessment). (d) Rhesus data for 48-h post-exposure damage using a 0.327-mm beam diameter from Ref. 10 (solid line, 458-nm thresholds; dashed line, 441-nm thresholds).

point (100 s), the 442-nm data in Fig. 3(b) deviate from the trends just discussed. In general, this biphasic response to changing laser exposure duration has been observed for damage at wavelengths shorter than 580 nm [see Fig. 3(b)] and has been used as an indicator of the transition from photothermal to nonthermal (photochemical) damage mechanisms. As shown in Fig. 3(a), this biphasic response had not occurred within the 100-s duration limit of our experiment when the RPE cells contained the higher density of MPs.

A comparison of Figs. 3(a)–3(d) provides support to the validity of the *in vitro* model when using 160 MPs/cell. The transition to irradiance reciprocity, and thus the presumed transition from photothermal to photochemical damage mechanisms, occurred in both the *in vivo* and *in vitro* models at exposure durations of about 10 s in the data for wavelengths of 488 nm and shorter. Of interest is the comparison for exposure to 514 nm. The *in vitro* data suggest that damage

Table 3 Power function equations describing the "linear" portions (log-log plot) of the temporal action profiles found in Fig. 3.

	160 MP/cell 0.1–10 s	160 MP/cell 1–100 s	1600 MP/cell 1–100 s	Ham[a] 1–16 s	Gibbons[b] 1–120 s
532 nm	$H=489(t^{0.86})$	$H=476(t^{0.82})$	$H=62(t^{0.88})$		
514 nm	$H=353(t^{0.83})$	$H=348(t^{0.81})$	$H=65(t^{0.85})$	$H=15(t^{0.88})$	$H=4631(t^{0.87})$
458 nm	$H=332(t^{0.86})$		$H=71(t^{0.88})$	$H=5(t^{0.83})$	
413 nm	$H=241(t^{0.84})$				

$R^2=1.00$ for all.
[a]Reference 2.
[b]Reference 8.

from 514 nm continues to be predominately thermal even at 100 s, whereas the data from Ham et al.[2] indicate irradiance reciprocity. Gibbons and Allen[8] have shown that, using Probit ED_{50} analysis in the rhesus model, 514 nm is a pivotal wavelength for achieving photochemical damage. Figure 3(c) shows that Gibbons and Allen[8] found reciprocity when assessing for damage at 24 h post exposure (latency), but not after 1 h post exposure. We interpret these results to indicate that the energy of photons at 514 nm is sufficient to achieve photochemical damage, but the mechanism of injury is dictated by the time interval chosen for damage assessment. Even though our spot size (250 μm) differs from that in the Gibbons and Allen study (estimated from Ref. 8 to be 50 μm), our 1 h post-exposure data (trend) for damage from exposure to 514 nm appear to fall in line with the animal model.

Even though differences in spot size and damage assessment led to disparate damage thresholds in both of the *in vivo* methods summarized in Fig. 3(c), the overall trends in their temporal action profile remain similar. Another means of comparing threshold trends is curve fitting of the data in temporal action profiles. The slope (exponent) of the "linear" portion (log-log plot) of pertinent curves in Fig. 3 compared favorably across the *in vivo* and *in vitro* (160 MPs/cell) methods (Table 3).

We have included in our Fig. 3(d) the 327-μm laser diameter data from the *in vivo* study of Lund et al.,[10] which represent exposure durations of 1 to 100 s (441 nm) and 0.1 to 100 (458 nm) at a spot size similar to that used both here and in Ham's studies[1,2,11] (500 μm). One of the conclusions made by Lund et al.[10] was that, even though their 458-nm thresholds were in good agreement to those of Ham et al.,[2] their 441-nm data differed at exposure durations shorter than 100 s. The newer study, which used a HeCd laser with greater power than was available when Ham et al.[2] did their study, now provides trusted data for the 441/442-nm wavelength and shows the expected temporal action profile trend (the break point for reciprocity and higher threshold values).

The trends in the temporal action profile of Fig. 3(d) are similar to the trends seen for 458 and 413 nm in Fig. 3(a). Not only is there an apparent transition from photothermal to photochemical damage at around the 10-s exposure time, the transitions are not as smooth, as depicted in Figs. 3(b) and 3(c) for 458 nm and longer. The interesting drop from the 413-nm radiant exposure threshold at 20 s (3640 J/cm^2) to that at 100 s in the *in vitro* model shown in Fig. 3(a) is similar to the 441-nm data seen in Fig. 3(d).

It should be noted, however, that Fig. 3(d) represents thresholds for damage assessed 48 h post exposure, and the threshold results for 1 h post exposure reported by Lund et al.[10] did not indicate irradiance reciprocity. This delayed appearance of damage at reduced irradiances is one characteristic used to distinguish thermal from nonthermal damage mechanisms (reviewed in Ref. 12). So it was interesting to find that irradiance reciprocity was shown after only 1 h in the *in vitro* model. Pigmentation could play a role in this difference between the two models. Figure 3(a) shows how increasing pigmentation 10-fold in our RPE cells caused a loss of irradiance reciprocity at 458 nm for 100-s exposures. Although the number per cell of MPs is about the same for the cell and animal models, the shape and spacing of cells differ in culture and the retina, making the MPs per unit area different. Perhaps lesion formation at 1 h post exposure at 458 nm in the eye has a major photochemical component. Maybe the environment of cultured cells (lack of tissue above and below) allows for more efficient dissipation of heat. We have addressed the issue of heat dissipation during exposures of cultured RPE at 413 nm using computer simulations of ED_{50} irradiances and found significant heating during exposures of 0.1 s, but not 100 s.[13]

Another plausible explanation for the lack of latency *in vitro* is one that accounts for the type of damage detected. The *in vitro* model, as described, uses an overt form of damage (plasmalemma breach) as the end point. Although one would expect the response to photo-damage in the eye to be a complex physiological process involving multiple tissue types, the delayed onset of a visible lesion is indicative of an apoptotic pathway. At present, issues of cell viability and overcrowding preclude our use of analyses for laser damage beyond 1 h post exposure, so an analysis for delayed onset of damage (apoptosis) of 24 to 48 h is not feasible. We are currently implementing methods of detecting biochemical traits that manifest at different times during the early stages of programmed cell death, which would make detection of apoptosis at 24 to 48 h post exposure unnecessary. We would look for irradiance reciprocity at each of those times post exposure (100-s exposure at 413 nm) and determine if increasing pigmentation in our cultured cells would generate the effect required to cause latency in the appearance of damage.

Although latency in damage detection is indicative of photochemical processes, we believe that the underlying principle of irradiance reciprocity is an equally definitive indicator. We do expect, therefore, a greater burst of photochemical oxidation *in vitro* (1-h assessment of membrane breach) than the animal model (48-h assessment of apoptosis). The significance of the similar trends (wavelength and exposure duration) for irradiance reciprocity in the cell and animal models was the motivation for additional studies. We have recently completed an ED_{50} analysis (with computer simulations) at 413 nm with varying exposure durations between 10 and 200 s that has begun to address some of the questions surrounding the transition in damage mechanisms from photothermal to photochemical.[13]

One inference from our analyses is that comparisons of threshold trends with respect to wavelength and exposure duration are useful for studying laser bioeffects, provided the method of damage assessment is consistent within the data set. For example, Payne et al.[9] used an artificial retina model (*in vitro*) to replicate the *in vivo* trends in damage (minimum visible lesions in rhesus) from ultrashort laser pulses when a melanosome-based (*in vitro*) or *ex vivo* (RPE and choroid explant) model could not. In this case, because the artificial retina included a depth of water approximating the length of a rhesus eye, the same degree of nonlinear self-focusing of the ultrashort pulses occurred in both.

We are presently using methods for *in vitro* laser exposure where temperature and humidity are controlled. This has led to a level of consistency in damage assessment necessary for accurate mathematical modeling of rate processes for both photothermal and photochemical damage. Using our *in vitro* data, we are beginning to incorporate photochemical rate pro-

cesses into traditional thermal models in the hopes of generating a universal laser damage model.

4 Conclusions

The described *in vitro* retinal model, with about 160 MPs/cell, accurately depicts how wavelength and exposure duration influence ocular laser damage in an animal model. The ranges of exposure duration and wavelength in which the apparent transition from photothermal to photochemical damage occurs (10 to 100 s and 458 to 514 nm, respectively) are consistent between the *in vitro* and *in vivo* models. The pigment dependence of these trends for photochemical damage in vitro corroborates the conclusions of Ham et al.[11] regarding the involvement of melanin in actinic damage processes in the retina.

Although the current description is provided as an example of how the model can be used in studying dose response, we do not presume to present a complete mapping of the parameter space available. Additional wavelengths and exposure durations, as well as the effects of laser diameter on thermal damage, are all interesting parameters to pursue in future studies of the *in vitro* model. Our current results support the idea that the *in vitro* RPE cell model can be used to study the effects of pigmentation, lipofuscin, and a host of environmental factors as they relate to the described baseline response behavior. The cell model will facilitate studies on cellular response to lasers, such as oxidation, effects of aqueous interfaces, exact inflections between damage mechanisms, and molecular profiling (transcriptomics and proteomics).

Acknowledgments

Any opinions, interpretations, conclusions, and recommendations are not necessarily endorsed by the U.S. Air Force. We thank H. Hodnett and D. Stolarski for technical assistance. This work was supported by the Air Force Office of Scientific Research (Grant No. 92HE04COR).

References

1. W. T. Ham Jr., J. J. Ruffolo Jr., H. Mueller, and D. Guerry III, "The nature of retinal radiation damage: dependence on wavelength, power level and exposure time," *Vision Res.* **20**, 1105–1111 (1980).
2. W. T. Ham Jr., H. A. Mueller, M. J. Ruffolo Jr., and A. M. Clarke, "Sensitivity of the retina to radiation damage as a function of wavelength," *Photochem. Photobiol.* **29**, 735–743 (1979).
3. D. J. Finney, *Probit Analysis*, Cambridge University Press, New York (1971).
4. C. P. Cain, G. D. Noojin, and L. Manning, "A comparison of various probit methods for analyzing yes/no data on a log scale," USAF School of Aerospace Medicine, Brooks Air Force Base, TX, USAF Technical Report AL/OE-TR-1996-0102 (1996).
5. M. L. Denton, M. S. Foltz, L. E. Estlack, D. J. Stolarski, G. D. Noojin, R. J. Thomas, D. Eikum, and B. A. Rockwell, "Damage threshold for exposure to NIR and blue lasers in an *in vitro* RPE cell system," *Invest. Ophthalmol. Visual Sci.* **47**, 3065–3073 (2006).
6. M. L. Denton, M. S. Foltz, K. J. Schuster, L. E. Estlack, and T. J. Thomas, "Damage thresholds for cultured retinal pigment epithelial cells exposed to lasers at 532 nm and 458 nm," *J. Biomed. Opt.* **12**, 034030 (2007).
7. M. L. Denton, M. S. Foltz, K. J. Schuster, L. E. Estlack, H. M. Hodnett, G. D. Noojin, and R. J. Thomas, "An in vitro model for retinal laser damage," in *Optical Interactions with Tissue and Cells XVII*, S. L. Jacques and W. P. Roach, Eds., *Proc. SPIE* **6435**, 643514 (2007).
8. W. D. Gibbons and R. G. Allen, "Retinal damage from long-term exposure to laser radiation," *Invest. Ophthalmol. Visual Sci.* **16**, 521–529 (1977).
9. D. J. Payne et al., "Comparative study of laser damage threshold energies in the artificial retina," *J. Biomed. Opt.* **4**, 337–344 (1999).
10. D. J. Lund, B. E. Stuck, and P. Edsall, "Retinal injury thresholds for blue wavelength lasers," *Health Phys.* **90**, 477–484 (2006).
11. W. T. Ham Jr., J. J. Ruffolo Jr., H. A. Meuller, A. M. Clarke, and M. E. Moon, "Histologic analysis of photochemical lesions produced in rhesus retina by short-wavelength light," *Invest. Ophthalmol. Visual Sci.* **17**, 1029–1035 (1978).
12. B. E. Stuck, "The retina action spectrum for photoretinitis ("blue-light hazard")," in *Measurements of Optical Radiation Hazards*, D. Sliney, Ed., pp. 193–208, Maerkl-Druck, München (1998).
13. M. L. Denton, M. S. Foltz, K. J. Schuster, C. D. Clark III, L. E. Estlack, and R. J. Thomas, "An in vitro model reveals a sharp transition between laser damage mechanisms," unpublished manuscript.